



Deformed Neutron Shells in the Symmetric Modal Fission of Pre-Actinides

S.I. Mulgin (INP), K.-H. Schmidt (GSI), A. Grewe (THD), S.V. Zhdanov (INP)

(INP) *Institute of Nuclear Physics, National Nuclear Centre,
480082 Almaty, Kazakhstan*

(GSI) *Gesellschaft für Schwerionenforschung, Planckstrasse 1,
64291 Darmstadt, Germany*

(THD) *Institut für Kernphysik, Technische Universität Darmstadt,
Schlossgartenstrasse 9, 64289 Darmstadt, Germany*

Abstract

An analysis of fragment mass distributions in the low-energy fission of nuclei from ^{187}Ir to ^{213}At has shown that shell effects in symmetric mode fragment mass yields of these nuclei could be interpreted as an influence of two strongly deformed neutron shells in arising fragments with neutron numbers $N_1 \approx 52$ and $N_2 \approx 68$. A new method has been proposed for quantitative describing the mass distributions of a symmetric fission mode for pre-actinides with $A \approx 180 \div 220$.

1. INTRODUCTION

Experimental investigations of fragment spectra in the low-energy fission of pre-actinide nuclei with atomic numbers $A = 187 - 213$ initiated by Prof. G.N. Smirenkin during the last decade [1-6] have shown that mass and energy distributions (MED) of fragments from the fission of these nuclei are modulated by sharply expressed irregularities conditioned by the influence of shell structure on the process of fragment formation. A very interesting manifestation of these effects takes place in a range of masses close to $A/2$.

However, these investigations did not answer the question about the nature of the shells-correction origin, particularly the question about the role played by the numbers of neutrons N and protons Z for the formation of these shell effects in a fissioning nucleus and in arising fragments, and what "magic" numbers Z and N are responsible for these shell corrections.

In order to clear the question up we have performed a combined analysis of all available experimental data on the MED of pre-actinide nuclei. In the course of this, the following problems were solved simultaneously:

1. The determination of shell-correction characteristics ("magic" values N and Z , typical deformation, and amplitude) which are responsible for the shell effects in the fragment yields of the symmetric fission mode for pre-actinide nuclei.

2. The development of a semicempirical method for describing symmetric mode mass yields in a range of nuclei with $A \approx 180 - 220$.

2. QUANTITATIVE CONSIDERATION

As it was outlined in investigations of fission-fragment angular distributions [8], pre-actinides have very large deformations of nuclei in the transition states. According to calculations within different versions of the liquid-drop model [9-11], configurations and potential energies at the saddle are close to those in the scission point. Proceeding from this, we suppose that the influence of dynamic effects on the descent from fission barrier to scission point is comparatively small, and therefore, the formation of the MED is generally defined by deformation potential energy landscape in the vicinity of the saddle point. As an evidence in favour of this hypothesis one can point out the investigations [3, 12] of mass-distribution dispersions – σ^2_m and the successful application of the transition-state method to describe fragment mass yields [2, 13].

Thus, we further suppose that the dependencies $Y(m)$, $E_k(m)$ and $\sigma^2_E(m)$ for pre-actinide nuclei directly reflect the dependencies of potential energy and deformation on mass-asymmetric coordinate of a fissioning nucleus. The manifestation of shell effects in the MED of pre-actinide nuclei is demonstrated in fig. 1, where the distributions $Y(m)$, $E_k(m)$ and $\sigma^2_E(m)$ are shown for nuclei from ^{187}Ir to ^{213}At at an excitation energy $U \approx 10$ MeV ($U = E^* - B_f$ – is the excitation energy above the fission barrier B_f).

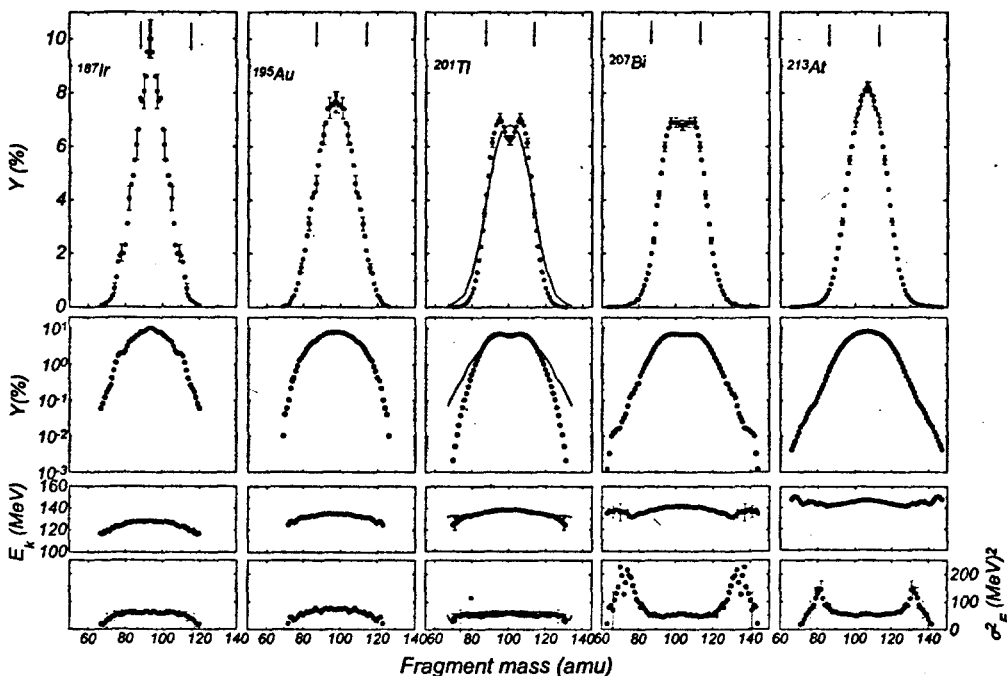


Fig. 1. Relative yields Y , total kinetic energies E_k and kinetic energy dispersions σ^2_E as a function of fragment mass. The experimental data points (\bullet) correspond to fission at excitation energy $U \approx 10$ MeV; arrows point out positions of proposed neutron shells, for ^{201}Tl the lines show in addition the experimental data taken at $U \approx 25$ MeV

This figure shows that the MED for ^{207}Bi and ^{213}At at $m \geq 127$ have sharply expressed irregularities. This phenomenon has been studied in detail in Refs. [1-3], where it was demonstrated that for nuclei heavier than ^{201}Tl the distributions $Y(m)$, $E_k(m)$ and $\sigma^2_E(m)$ consist of the MED of three independent fission modes:

1. The symmetric fission mode due to strongly elongated shapes of the fissioning nucleus throughout the trajectory of descent from fission barrier to scission point and comparatively low values of the fragment kinetic energies.
2. The asymmetric mode (Standard I, in terms of Ref. [7]), conditioned by shells in the heavy fragments with deformations close to spherical ones and with masses close to 132.
3. A second asymmetric mode (Standard II), formed by shell effects in heavy fragments with comparatively small deformation and with masses close to 138.

In low-energy fission of pre-actinide nuclei, as it becomes clear from fig. 1, the shapes of the $Y(m)$ -distribution in the symmetric mode strongly depend on the nucleon composition of the fissioning nuclei and deviate significantly from Gaussian distributions predicted by the liquid-drop model. At the same time, at excitation energies $U \geq 25$ MeV, the mass-distribution $Y(m)$ for pre-actinide nuclei like ^{201}Tl (solid curves) becomes close to the Gaussian shape. Such behaviour of $Y(m)$ could be explained by the contribution of shell corrections to the potential energy of the saddle configurations and their influence on the arising fragments [4]. With increasing energy the influence of shell effects decreases, and $Y(m)$ goes toward the liquid-drop limit.

One should note that, generally speaking, it is necessary to consider the shell structure of a nucleus as a whole. But, the calculations within framework of the shell correction method [14, 15] and properties of heavy fragments of transactinide nuclei show that the shell structure of the whole nucleus in pre-scission configurations is essentially determined by shells in the arising fragments.

In contrast to $Y(m)$, the dependencies of $E_k(m)$ and $\sigma^2_E(m)$ in the symmetric mode conserve smooth liquid-drop behaviour at all excitation energies. Taking into account the direct connection between the energy distributions and the configurations of the fissioning nuclei, one can consider this circumstance as an argument that the deformations corresponding to these shells are close to the large deformations which are optimal for liquid-drop fission. Therefore, the shell effects in the fission of pre-actinide nuclei are conditioned by strongly deformed shells. This conclusion is supported by a good agreement between liquid-drop momenta of inertia and experimental ones [16].

In order to clear up the question about the influence of proton number Z and neutron number N on the shell effects in the symmetric fission of pre-actinides let us look at fig. 2 which presents the data on $Y(m)$ for fissioning nuclei with $Z=83 \div 85$ and $N=124 \div 128$ at $U \approx 10$ MeV.

One can see that at coinciding N and different Z the shapes of the distributions are practically the same (pairs $^{207}\text{Bi} - ^{208}\text{Po}$, $^{212}\text{Po} - ^{213}\text{At}$), but at coinciding Z and different N the shapes change very fast (^{208}Po , ^{210}Po , ^{212}Po). So, we suppose that namely the neutron number N in the arising light and heavy fragments plays a predominant role in the formation of shell effects. An analogous situation arises in the fission of

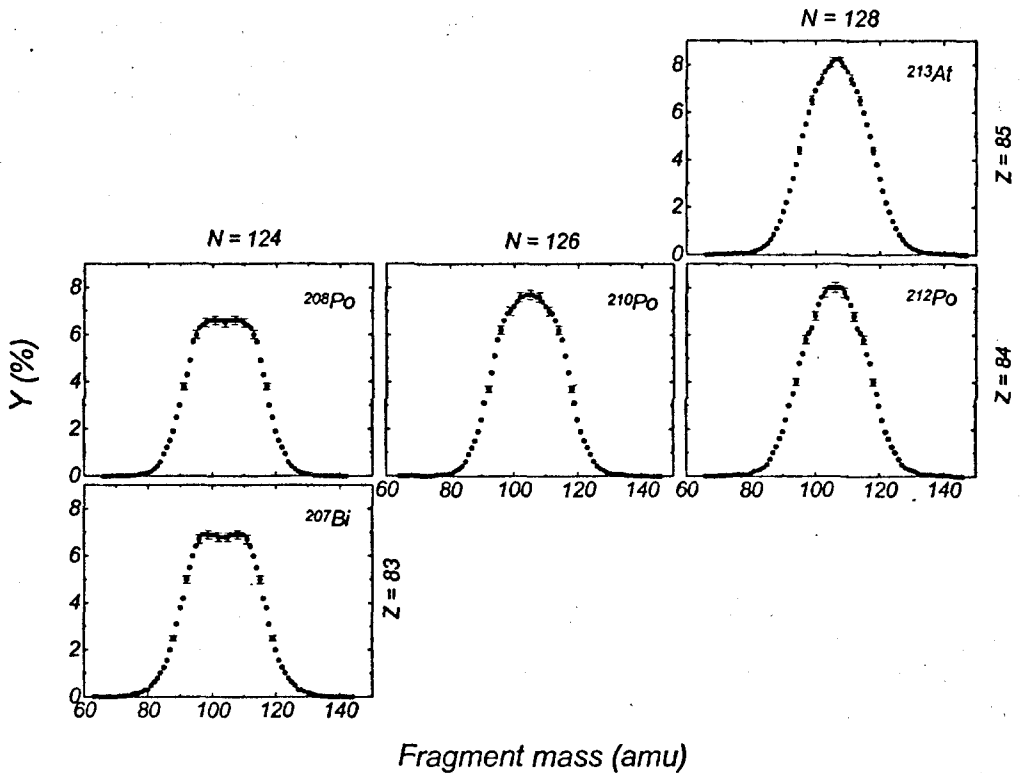


Fig. 2. Experimental relative yields Y versus fragment mass for nuclei from ^{207}Bi to ^{213}At at an excitation energy $U \approx 10$ MeV

heavier nuclei [17, 18], where a strong N -dependence of the shapes of the $Y(m)$ distributions is also observed. These experimental data have been explained within the shell-correction method, which demonstrates that for heavy nuclei the values of neutron shell corrections exceed those of the protons by a factor of two and even more.

Taking the above-mentioned properties of the symmetric fission mode as a basis, one can attempt to explain the alteration of $Y(m)$ -distribution shapes, presented in fig. 1, by the existence of two strongly deformed neutron shells with "magic" values $N_1 < 110/2$ and $N_2 > 128/2$, considering that ^{187}Ir has 110 neutrons and ^{213}At has 128 neutrons. In this case, for ^{187}Ir at $m \approx A/2$, the numbers of neutrons in the light and the heavy fragments are approximately equal ($N_L \approx N_H \approx 55$), and the N_1 -shells in the light and the heavy fragments add up. This increases the relative yield of fragments with $m \approx A/2$. At the same time, the influence of the N_2 -shell on $Y(m)$ is weaker, it just increases the yields in the tails of the distributions for heavy fragments with $m > 109$. In the fission of ^{213}At , the situation is reflecting, the N_2 -shell enhances the yield of fragments with $m \approx A/2$, and the N_1 -shell favours those of light fragments with $m < 91$. The appearance of sharply expressed two-humped distribution in the fission of ^{201}Tl could be explained within this approach in the following way. The

N_2 -shell enhances the yield of heavy fragments in the vicinity of masses $m_H \approx N_2 A/N$, and the N_1 -shell supports the yield of complementary light fragments with masses $m_L = (A - m) \approx N_1 A/N$, i.e. the shells N_1 and N_2 are located at approximately equal distances from $A/2$. This circumstance, altogether with relative symmetry of $Y(m)$ -shapes for nuclei around ^{201}Tl observed in fig. 1, allows to assume that there is a connection between N_1 and N_2 , namely $N_1 + N_2 \approx 120$, where 120 is the total number of neutrons in ^{201}Tl .

The hypothesis about existence of two strongly deformed neutron shells and the direct connection of the deformation potential energy of nuclei at the saddle point with $Y(m)$ -distribution became a basis of the proposed method for describing mass yields in the symmetric mode fission in the region of pre-actinides.

3. ANALYSIS METHOD

In order to describe the mass distributions we used the method outlined in the works of Moretto and co-workers [13, 19] and in our previous publications [2-6]. According to this approach, the yield of fragments with mass m is defined by the probability to overcome the conditional fission barrier $B_f(m)$ corresponding to this mass. Following the Bohr-Wheeler formula [20] and the approximation proposed by Moretto [19], one can evaluate relative fragment yields normalised to 200% by:

$$Y(m)/200\% \approx \exp[S_f(m)] / \sum_{m=0}^A \exp[S_f(m)]. \quad (1)$$

Here $S_f = 2\sqrt{aU} = 2a\theta$ is the entropy of the fissioning nucleus; $\theta = \sqrt{[E - B_f(m)]/a}$ - temperature of the fissioning nucleus; E - the excitation energy; a - the level density parameter in the transition state calculated according to [21, 22].

The height of the conditional fission barrier $B_f(m)$ is defined as the difference between the potential energies of the nucleus at the ground and at the transition state, and within the shell correction method could be evaluated as [23]:

$$B_f(m) = (B_f^{\text{LD}} - W_g) + \frac{8q}{A^2} \left(m - \frac{A}{2}\right)^2 + W_f(m). \quad (2)$$

Here B_f^{LD} - liquid-drop fission barriers $W_f(m)$ and W_g are the shell corrections in transition state (f) and ground state (g); q - the stiffness parameter of the liquid drop with respect to mass-asymmetric variations of the saddle shape.

Liquid-drop fission barriers B_f^{LD} and shell-correction values W_g were taken from the calculations of Myers and Swiatecki [9]. One should note that the calculated heights of fission barriers $B_f = B_f^{\text{LD}} - W_g$ are in a good agreement with the experimental values B_f [8].

In our approach, the shell correction W_f is defined as the sum of shell corrections in the light and the heavy fragments:

$$W_f(m) = W_H\left(m \frac{N}{A}\right) + W_L\left(N - m \frac{N}{A}\right) = W_H(N_H) + W_L(N_L). \quad (3)$$

The connection between N_H , H_L and "magic" numbers of shells N_1 , N_2 was established as:

$$\begin{aligned} W_H(N_H) &= \text{MIN}[F_1(N_H, N_1), F_2(N_H, N_2)] \\ W_L(N_L) &= \text{MIN}[F_1(N_L, N_1), F_2(N_L, N_2)] \end{aligned} \quad (4)$$

where the function MIN selects the minimum value of F_1 and F_2 . The functions F_i ($i = 1, 2$) which describe the dependencies of correction amplitudes on the number of neutrons in the fragment were parametrised by the simplest parabolic equations:

$$F_i(N, N_i) = \begin{cases} \beta_i \left[1 - (N - N_i)^2 / \alpha_i^2 \right] \\ 0, \text{ at } F_i \geq 0 \end{cases} \quad (5)$$

So, the Eqs. (1) - (5) show that in order to describe the $Y(m)$ -distributions, it is necessary to find a method to determine the values of the liquid-drop stiffness parameter q for a given nucleus and the shell parameters N_i , α_i and β_i ($i = 1, 2$) which are common for all pre-actinide nuclei.

With this aim we have analysed 30 experimental $Y(m)$ -distributions for fissioning nuclei from ^{187}Ir to ^{213}At in a range of excitation energies $U = 7 \div 25$ MeV. These data were described with Eqs. (1) - (5), and values of above-mentioned description parameters were determined within the least squares' method (the χ^2 - method) using the code MINUIT [24]. The evaluation of these distributions was constrained so that the parameters N_i , α_i and β_i are common for all distributions, and the parameter q can change for different nuclei. It should be noted that q is characteristic for the liquid-drop potential of a given nucleus and does not depend on an excitation energy U . Nevertheless, in our analysis of $Y(m)$ -distributions measured for the same nucleus at different excitation energies we allowed the parameter q to change within limits of $\pm 5\%$. These variations enable to take into account possible experimental errors of experimental data which, for the values $\sigma_m^2 \sim 1/q$, amount to about 5% [3, 25].

4. RESULTS AND DISCUSSION

The resulting descriptions of the $Y(m)$ -distributions for 9 nuclei at $U \approx 10$ MeV are presented in fig. 3 where calculations are shown by solid curves, and experimental data correspond to open circles. From this figure one can see that the proposed approach allows to reproduce the sharp alterations of the individual shapes of the distributions at different nucleon compositions of the fissioning nuclei. Local distinctions between the experimental results and their description in $Y(m)$ do not exceed two standard deviations.

Taking into account the very simplified parametrization of $F_i(N, N_i)$, the neglect of the proton shell contributions, and other approximations of the method, one should admit that the quality of the mass yield description in dependence on Z and N of the fissioning nuclei is astonishing enough.

The description of the U -dependence of mass yields $Y(m)$ is shown in fig. 4 for ^{201}Tl , for example. This figure demonstrates that the achieved description of temperature damping of the shells allows to reproduce the gradual transition of the experimental mass yields $Y(m)$ to Gaussian-like distributions at $U > 25$ MeV.

As it was pointed out above, one of the objectives of our work is to design a method for determining the dependence of the liquid-drop stiffness parameter q on the nucleon composition of a given fissioning nucleus. With this aim, the optimal values $q = A^2/16 \cdot d^2V/d\eta^2$ found in the analysis are presented in fig. 5 (closed circles) in their dependence on the fissility parameter Z^2/A . Open circles show the data on $d^2V/d\eta^2$ obtained by another independent method. Namely on the base of the analysis of mass dispersions σ_m^2 measured in the high-energy fission induced by light charged particles and heavy ions [25]. This figure demonstrates that within limits of experimental scattering of the data both sets of data on $d^2V/d\eta^2(Z^2/A)$ coincide. This is a good agreement in favour of the method proposed in the present work. So, we recommend to use the smooth description (solid curve in fig. 5) of the dependence $d^2V/d\eta^2(Z^2/A)$ obtained by Rusanov and co-workers [25].

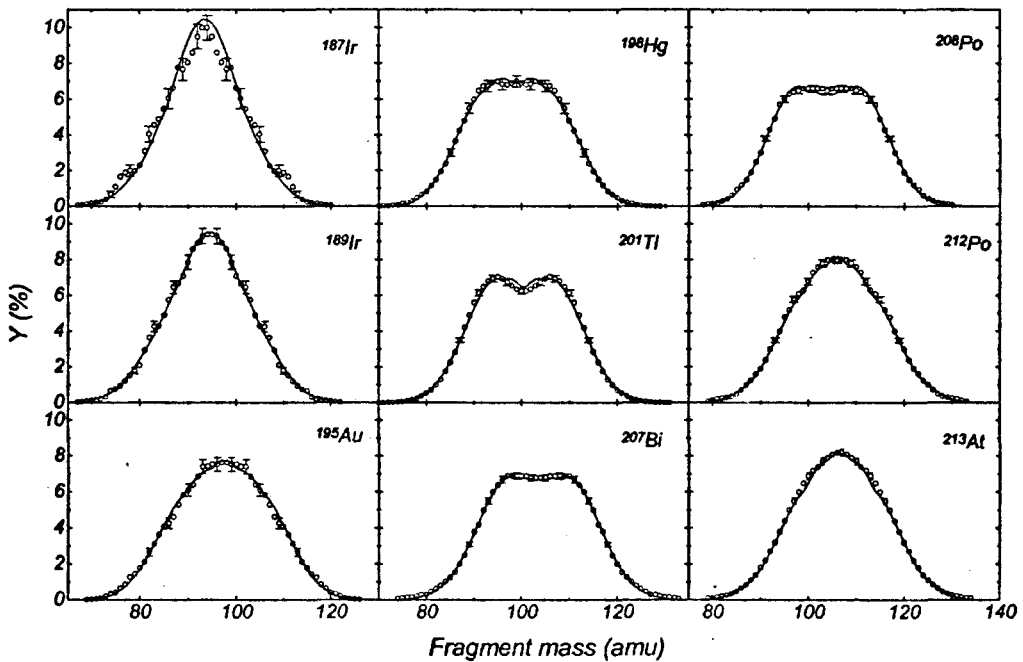


Fig. 3. Relative yields Y and their description versus fragment mass for nuclei from ^{187}Ir to ^{213}At at an excitation energy $U \approx 10$ MeV. The experimental data (o) and the proposed description (—) are shown

The shell parameters used for the description of the experimental data of fig. 3 are represented in table 1:

Table 1. Parameters of the shell description

N_1	51.5	N_2	68.3
α_1	8.1	α_2	5.6
β_1	-0.37	β_2	-0.19

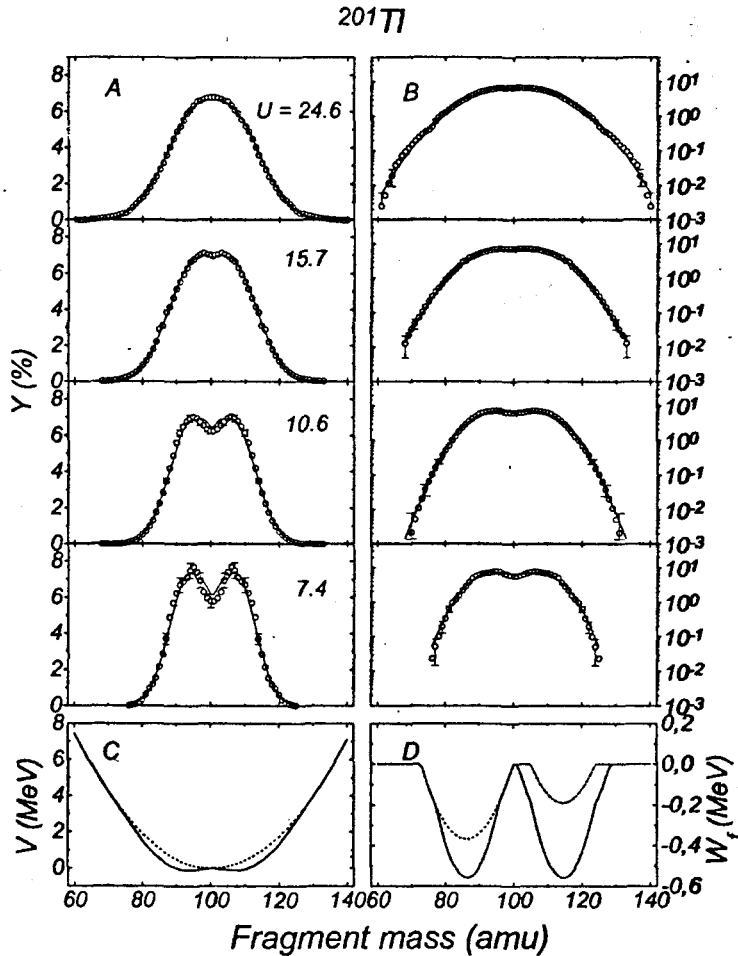


Fig. 4. Relative yields Y , their description, calculated potential energy and its constituents versus fragment mass for ^{201}Tl at different excitation energies. Part "A": (o) the experimental yields Y and (—) the proposed description in a linear scale; part "B": (o) the experimental yields Y and (—) the proposed description in a logarithmic scale; part "C": full (—) and liquid-drop (---) potential energies; part "D": calculated shell corrections in the light fragment group W_L (---), in the heavy fragment group W_H (— · —), and for the whole nucleus W_f (—)

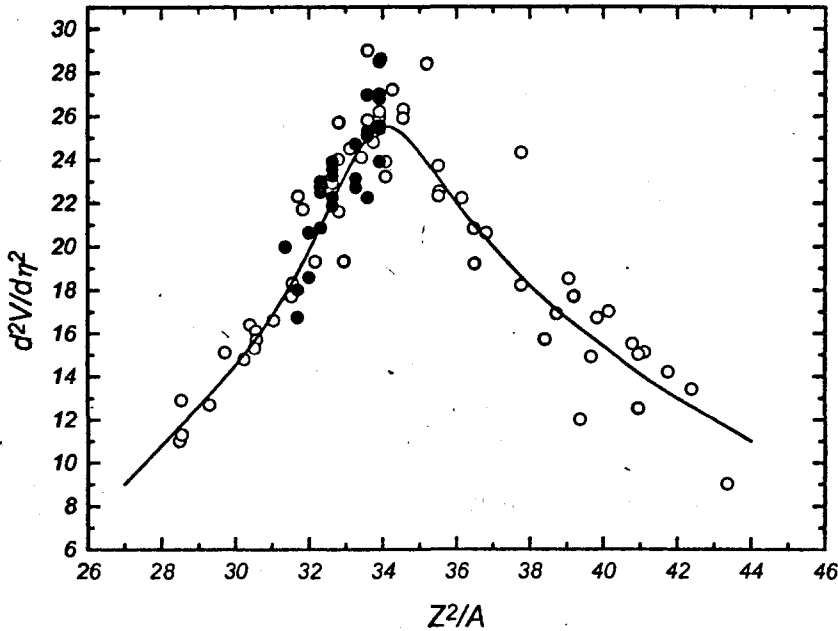


Fig. 5. The liquid-drop stiffness with respect to mass-asymmetric deformations at the saddle point $d^2V/d\eta^2$ in the dependence on the fissility parameter Z^2/A . (●) The optimal values found in our analysis for nuclei from ^{187}Ir to ^{213}At at excitation energies $U \approx 7\text{--}25$ MeV, (○) experimental values and (—) their description from Ref. [25]

The fragment-mass dependencies of the liquid-drop (dashed curves) and full (solid curves) deformation potential energies calculated with these parameters for the nucleus ^{201}Tl are shown in part "C" in fig. 4. Part "D" in this figure demonstrates the dependencies $W_L(m)$ and $W_H(m)$ for light (dashed curve) and heavy (dashed-dotted curve) fragments, respectively, and also the dependencies of $W_f(m)$ for a nucleus as a whole (solid curve). One can see that, though the contribution of shell constituents to the full potential energy of a nucleus is comparatively small, it visibly influences on the shapes of the $Y(m)$ -distributions.

Coming back to table 1, we should note that the extracted "magic" neutron numbers N_1 and N_2 are close to the neutron shells $N \approx 52$ and $N \approx 68$ appearing at very large deformations in the calculations of neutron shell corrections performed by Wilkins and co-workers [26] ($\beta \approx 1$) and by Moreau and co-workers [27] ($\epsilon \approx 0.9$). On the other hand, these shells are not observed in the calculations carried out by Ragnarsson and Sheline [28]. Unfortunately, one could not expect something certain from the direct comparison of our results with the existing theoretical systematics of shell corrections, since having considered the average total kinetic energies and the effective momenta of inertia, one can judge only about the deformation of a nucleus as a whole, but not about the shapes of arising fragments taken separately, because of the same kinetic energies and momenta of inertia could be provided by essentially different combinations of shapes of the arising fragments and the length of the neck be-

tween them. However, it is clear that "effective" deformation of these shells essentially exceeds the deformations of the shells which are responsible for Standard I and Standard II and is close to the liquid-drop one.

An additional evidence of the existence of the shells with $N_1 \approx 52$ and $N_2 \approx 68$ was obtained in describing $Y(m)$ within the least squares' method by means of more flexible poly-parametric functions for $F_i(N, N_i)$ like Sharlie distributions or asymmetric functions mathematically similar to Woods-Saxon potential, for example. This calculations showed that the parameters N_1 , N_2 and q extracted by using the above-mentioned functions practically coincide with those found for parabolic dependencies.

At the same time, effective parameters of shell amplitudes and widths (analogous to the parameters α and β for a parabola) visibly (up to 20 %) differed from each other and from the values given in table 1. These distinctions point out that our analysis does not allow to make decisive conclusions about details of the functions $F_i(N, N_i)$. This limits the predictive power of the proposed approach to the description of $Y(m)$ -distributions. Taking this limitation into consideration, we recommend to use the parameters of table 1 for the description of the symmetric fission mode only for nuclei within the limits $A \approx 180 \div 220$.

5. CONCLUSIONS

Shell effects in the symmetric mode of fragment mass yields from the fission of pre-actinide nuclei from ^{187}Ir to ^{213}At could be explained and described if one assumes the existence of two strongly deformed neutron shells in the arising fragments with neutron numbers $N_1 \approx 52$ and $N_2 \approx 68$.

A new method has been proposed for quantitative describing the mass distributions $Y(m)$ of the symmetric mode in the fission of pre-actinides with $A \approx 180 \div 220$.

REFERENCES

1. Itkis M.G. et al., *Yad. Fiz.* 41 (1985) 849 (*Sov. J. Nucl. Phys.* 41 (1985) 544).
2. Itkis M.G. et al., *Yad. Fiz.* 43 (1986) 1125 (*Sov. J. Nucl. Phys.* 43 (1986) 719).
3. Itkis M.G. et al., *Particles and Nuclei, JINR, Dubna, Moscow, Atomizdat.* 19 (1988) 701 (*Sov. J. Part. Nucl.* 19 (1988) 301).
4. Itkis M.G. et al., *Yad. Fiz.* 47 (1988) 7 (*Sov. J. Nucl. Phys.* 47 (1988) 4).
5. Itkis M.G. et al., *Yad. Fiz.* 52 (1990) 944 (*Sov. J. Nucl. Phys.* 52 (1990) 601).
6. Itkis M.G. et al., *Yad. Fiz.* 53 (1991) 1225 (*Sov. J. Nucl. Phys.* 53 (1991) 757).
7. Brosa U. Et al., *Phys. Rep.* 194 (1990) 167.
8. Ignatyk A.V. et al., *Particles and Nuclei, JINR, Dubna, Moscow, Atomizdat.* 16 (1985) 709 (*Sov. J. Part. Nucl.* 16 (1985) 307).
9. Myers W.D. and Swiatecki W.J. *Arkiv. Fys.* 36 (1967) 343.
10. Strutinsky V.M. *Yad. Fiz.* 1 (1965) 821 (in Russian)
11. Krappe H.J. et al., *Phys. Rev.* C20 (1979) 992.
12. Gruzintsev Ye.N. et al., *Z. Phys.* A323 (1986) 307.

13. McMahan M.A. et al., Phys. Rev. Lett. 54 (1985) 1995.
14. Brack M. et al., Rev. Mod. Phys. 44 (1972) 320.
15. Pashkevich V.V. Nucl. Phys. A169 (1971) 275.
16. Beizin S.D. et al., Yad. Fiz. 43 (1986) 1373 (Sov. J. Nucl. Phys. 43 (1986) 883).
17. Steinhäuser S. Et al., Proc. "Dynamical Aspects of Nuclear Fission", J. Kliman (Ed.), B. I. Pustyl'nik (Ed.) in Casta-Papiernicka, Slovak. Rep., (JINR, Dubna) (1996) 151..
18. Itkis M.G. et al., Proc. XV. ESP. Nucl. Phys. Div. on Low Energy Nuclear Dynamics 1995, St. Petersburg (World Scientific, Singapore), (1995) 177.
19. Moretto L.G. Nucl. Phys. A247 (1975) 211.
20. Bohr N. and Wheeler J. A. Phys. Rev. 56 (1939) 426.
21. Ignatyk A.V. Statistical properties of excited nuclei. Moscow, Energoizdat. (1983) (in Russian).
22. Ignatyk A.V. et al., Yad. Fiz. 29 (1986) 875 (Sov. J. Nucl. Phys. 29 (1986) 450).
23. Strutinsky V.M. JETF 60 (1963) 1900 (in Russian).
24. CERN Computer 6600 series program Library Long-Write-UP "MINUIT".
25. Rusanov A.Ya. et al., Yad. Fiz. 60 (1997) 773 (Phys. At. Nucl. 60 (1997) 683).
26. Wilkins B.D. et al., Phys. Rev. C14 (1976) 1832.
27. Moreau J. Et al., Proc. Journées d'Etudes sur la Fission, Archachon. Report CENBG 8722. CEN Gradignan, France (1987) C1.
28. Ragnarsson J. and Sheline R. K. Physika Scripta 29 (1984) 385.